

# An ART iterative reconstruction algorithm for computed tomography of diffraction enhanced imaging<sup>\*</sup>

WANG Zhen-Tian(王振天)<sup>1,2</sup> ZHANG Li(张丽)<sup>1,2</sup> HUANG Zhi-Feng(黄志峰)<sup>1,2;1)</sup>  
KANG Ke-Jun(康克军)<sup>1,2</sup> CHEN Zhi-Qiang(陈志强)<sup>1,2</sup> FANG Qiao-Guang(方侨光)<sup>1,2</sup>  
ZHU Pei-Ping(朱佩平)<sup>3</sup>

1 (Department of Engineering Physics, Tsinghua University, Beijing 100084, China)

2 (Key Laboratory of Particle & Radiation Imaging (Tsinghua University), Ministry of Education, Beijing 100084, China)

3 (Beijing Synchrotron Radiation Facility, Institute of High Energy Physics, Chinese Academy of Sciences, Beijing 100049, China)

**Abstract** X-ray diffraction enhanced imaging (DEI) has extremely high sensitivity for weakly absorbing low- $Z$  samples in medical and biological fields. In this paper, we propose an Algebra Reconstruction Technique (ART) iterative reconstruction algorithm for computed tomography of diffraction enhanced imaging (DEI-CT). An Ordered Subsets (OS) technique is used to accelerate the ART reconstruction. Few-view reconstruction is also studied, and a partial differential equation (PDE) type filter which has the ability of edge-preserving and denoising is used to improve the image quality and eliminate the artifacts. The proposed algorithm is validated with both the numerical simulations and the experiment at the Beijing synchrotron radiation facility (BSRF).

**Key words** diffraction enhanced imaging, algebra reconstruction technique, phase contrast imaging

**PACS** 42.30.Wb, 42.30.Va, 41.60.Ap

## 1 Introduction

In the last decade, due to the availability of new brilliant and coherent sources, hard X-ray phase contrast imaging methods have developed rapidly. Diffraction enhanced imaging (DEI) based on synchrotron radiation is a non-destructive testing and diagnostic technology which has an extremely high sensitivity for weakly absorbing low- $Z$  samples in medical and biological fields. The conception of the DEI was first developed by Chapman et al at the National Synchrotron Light Source (NSLS) in 1996<sup>[1]</sup>.

Compared with conventional computer tomography (CT), the projective data in computed tomography of diffraction enhanced imaging (DEI-CT) are the integral of the partial derivative of the refractive index of the sample along the beam path. When combined with reconstruction algorithms that reconstruct the refraction index distribution of the sample, DEI-CT can investigate the inner structure of a weakly absorbing sample. Dilmanian et al first realized the

DEI-CT based on the geometric optics approximation (GOA) method at the NSLS in 2000<sup>[2]</sup>. For parallel-beam, Pavlov et al proposed an indirect algorithm<sup>[3]</sup>: firstly restore the “directional derivative projections” to the line integral of the refraction index decrement  $\delta$ , and then reconstruct  $\delta$  by the filtered backprojection (FBP) algorithm. Maksimenko et al presented another indirect algorithm<sup>[4]</sup>: firstly reconstruct  $\nabla\delta$  and restore  $\delta$  using an integrating method. Huang et al presented a direct FBP type algorithm to solve the reconstruction problem in the parallel-beam case<sup>[5]</sup>. Zhu et al advised a reconstruction framework to reconstruct the gradient of the refraction index according to the DEI layout of the Beijing Synchrotron Radiation Facility (BSRF)<sup>[6]</sup>.

Liu et al proposed a maximum likelihood iterative algorithm for DEI reconstruction<sup>[7]</sup>. He applied a maximum likelihood iterative formula of emission CT (ECT) to DEI-CT based on a successful simulation of the imaging process. Poisson noise process was assumed. Compared with the analytical methods,

---

Received 17 December 2008, Revised 12 May 2009

<sup>\*</sup> Supported by National Natural Science Foundation of China (10875066) and Program for New Century Excellent Talents in University (NCET-05-0060)

1) E-mail: huangzhifeng@mail.tsinghua.edu.cn

©2009 Chinese Physical Society and the Institute of High Energy Physics of the Chinese Academy of Sciences and the Institute of Modern Physics of the Chinese Academy of Sciences and IOP Publishing Ltd

iterative reconstruction algorithms<sup>[7, 8]</sup> exhibit great advantages in noisy and few-view circumstances, as in the case of biological samples, to reduce the exposure time due to the absorbed dose consideration.

In this paper, an ART iterative algorithm named DEICT-ART is proposed to reconstruct the gradient of the refraction index of the sample. To improve the convergent speed, an Order Subsets technique is adopted to accelerate the iterative reconstruction. Few-view reconstruction of DEICT-ART is studied and a partial differential equation (PDE) type filter which has the ability of edge-preserving and denoising is used to eliminate the artifacts in the few-view reconstruction. Our algorithm is validated with both the numerical simulations and the experiments at the BSRF.

## 2 DEI-CT layout at BSRF

The algorithm and the actual experiment are based on the DEI setup at the 4W1A Beamline of the BSRF. The layout of the experimental setup is shown in Fig. 1 of Ref. [9]. It is composed of two perfect crystals: one acted as the monochromator and the other acted as the analyzer. A white beam from the synchrotron radiation source was monochromatized by the monochromator. The transmitted beam changed its direction of propagation slightly because of the refractive index's gradients of the sample. The refracted beam was diffracted by the analyser before the detector. The rocking curve (RC) of the double crystal system describes the reflectivity of the monochromator-analyzer system as a function of the incident angle. The refraction of the sample on the final projection data can be measured by the rocking curve through extraction methods<sup>[10]</sup>.

## 3 Review of Zhu's algorithm

Zhu et al proposed a framework to reconstruct the gradient of the refraction index<sup>[6]</sup>. The phase gradient contribution can be written as

$$\nabla\Phi(x, y) = \frac{2\pi}{\lambda} \int_{\text{sample}} \left[ \frac{\partial\delta}{\partial x} e_x + \frac{\partial\delta}{\partial y} e_y \right] ds, \quad (1)$$

where  $\delta$  is the refractive index decrement,  $\Phi(x, y)$  is the total phase change along the ray path,  $e_x$  and  $e_y$  are the unit vectors along the  $X$  and  $Y$  axes, respectively, and  $s$  is the ray path. According to the geometry of Fig. 1 in Ref. [9], when the sample is rotated along the axis  $Z$  with an angle  $\beta$ , Zhu et al

deduced that:

$$(\Delta\theta)_\beta \cos\beta = \int_{\text{sample}} \frac{\partial\delta}{\partial x} ds, \quad (2)$$

$$(\Delta\theta)_\beta \sin\beta = \int_{\text{sample}} \frac{\partial\delta}{\partial y} ds, \quad (3)$$

where  $(\Delta\theta)_\beta$  is the refraction angle when the rotating angle is  $\beta$ . After the refraction angle information is retrieved by the extraction methods, a conventional CT algorithm can be used to reconstruct the gradient of the refraction index. In this paper, only  $\frac{\partial\delta}{\partial x}$  is reconstructed for example.

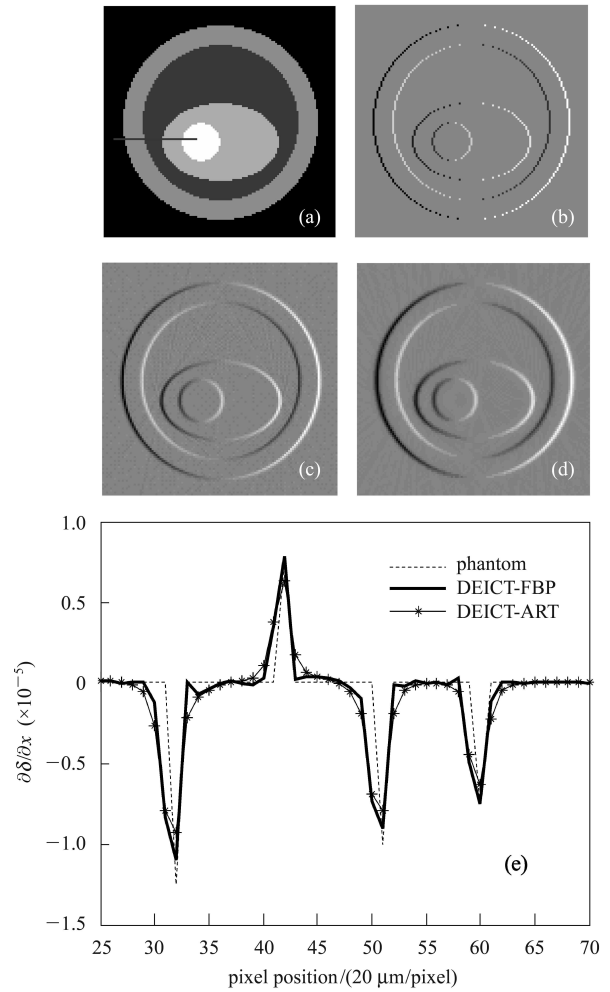


Fig. 1. Reconstruction results of the phase phantom. (a) The phase phantom; (b)  $\frac{\partial\delta}{\partial x}$  of the phantom to be reconstructed; (c) The reconstruction result of DEICT-FBP; (d) The reconstruction result of DEICT-ART; (e) Local profile comparison of the 70th row of the phantom indicated by the gray line in (a).

## 4 ART algorithm for DEI-CT

We propose that the ART iterative algorithm named DEICT-ART be taken to reconstruct the gradient of the refraction index instead of the widely-used FBP algorithm (DEICT-FBP). Compared with the analytical algorithm like FBP, the ART iterative algorithm has advantages in anti-noise and few-view reconstruction. Another attractive feature of the ART iterative approach is that it is possible to incorporate some types of a priori information into the solution. DEICT-ART inherits the advantages of ART.

The DEICT-ART algorithm proposed contains three steps:

1) Refraction angle extraction.

We use multiply-images statistical (MIS) method to extract the refraction angle<sup>[10, 11]</sup>. Two groups (a sample group and a background group) of DEI images are measured in several positions of the RC. The refraction-angle image is calculated on the pixel-by-pixel basis by Formula (4):

$$\begin{aligned}\theta_s &= \sum_n \theta_n I_s(n) / \sum_n I_s(n), \\ \theta_{bg} &= \sum_n \theta_n I_{bg}(n) / \sum_n I_{bg}(n), \\ \theta_{MIS} &= \theta_s - \theta_{bg},\end{aligned}\quad (4)$$

where  $I_s(n)$  and  $I_{bg}(n)$  denote the intensity of the DEI image in the position  $\theta_n$  of the RC with the sample and without the sample, respectively.

2) Refraction angle data preprocessing.

Preprocess the refraction angle projection data according to Zhu's algorithm:

$$p = (\Delta\theta)_\beta \cos \beta. \quad (5)$$

3) ART reconstruction.

A simultaneous ART formula proposed in Ref. [11] is adopted in the final reconstruction:

$$x_j^{k+1} = x_j^k + \frac{\sum_i \left[ a_{ij} \frac{p_i - \langle a_i, \hat{x} \rangle}{\sum_{j=1}^N a_{ij}} \right]}{\sum_i a_{ij}}, \quad (6)$$

where  $x_j^k$  is the  $j$ th pixel of the image vector  $\hat{x}$  in the  $k$ th iteration;  $p_i$  is the  $i$ th projection measured;  $a_{ij}$  is the contribution of the  $j$ th pixel to the  $i$ th ray;  $\langle a_i, x \rangle = \sum_j a_{ij} x_j$ , is a forward projection process ray

by ray.

Iterative algorithm suffers from the slow convergence. To accelerate the DEICT-ART algorithm, we use an ordered subsets (OS) technique. OS was first discussed in Ref. [12] for ART algorithm<sup>[13]</sup>, and more attention was paid to it after the concept was proposed by Hudson<sup>[14]</sup>. The basic idea is to use the orthogonality of the projection data to reduce the redundant information in the sequential projections. The formula of DEICT-OS-ART proposed is

$$\begin{cases} x_j^{k,m+1} = x_j^{k,m} + \frac{\sum_{i \in S_m} \left[ a_{ij} \frac{p_i - \langle a_i, \hat{x} \rangle}{\sum_{j=1}^N a_{ij}} \right]}{\sum_i a_{ij}}, \\ x_j^{k+1} = x_j^{k,M} \end{cases}, \quad (7)$$

where  $M$  is the number of subsets,  $m = 1, 2, \dots, M$  is the index of subsets and  $S_m$  is the  $m$ th subset.

## 5 PDE filter

Partial differential equations (PDE) in image modeling, denoising and edge-detection have grown significantly over the past few years. The PDE-based models modify an image with a PDE by looking for its solution. A PDE filter called anisotropic diffusion which was initially introduced by Perona et al<sup>[15]</sup> has the property of edge-preserving and denoising. Considering that the reconstructed object is the gradient of refraction index, the reconstruction images usually consist of sharp edges (at the edge of the sample where the refraction index changes greatly) and smooth regions (within the sample where the refraction index does not change or changes gradually). Based on this prior knowledge, PDE filter is suitable for image quality improvement and artifacts elimination of our reconstruction images.

Given an original image  $f$ , the anisotropic diffusion scheme proposed can be described by the following equation<sup>[15]</sup>:

$$\frac{\partial f}{\partial t} = \nabla \bullet (g(|\nabla f|) \nabla f), \quad (8)$$

$\nabla$  denotes the gradient operator,  $\nabla \bullet$  is the divergence operator, and  $|f|$  is the gradient magnitude of image  $f$ . If  $g(|\nabla f|)$  that has a high value at the smooth region of the image and a low value at the edge is chosen, the diffusion process is controlled to denoise while preserving edges.

One type of  $g(|\nabla f|)$  proposed by Perona et al is:

$$g(|\nabla f|) = \frac{1}{1 + (|\nabla f|/\sigma)^2}, \quad \sigma > 0, \quad (9)$$

where  $\sigma$  is a user-defined threshold that controls the edge sensitivity. The iterative PDE filtering method is:

$$f^{l+1} = f^l + \Delta t \times \nabla \cdot (g(|\nabla f|)\nabla f), \quad (10)$$

where  $l$  is the index of the filtering iteration and  $\Delta t$  is the step size which decides the stability of the filtering<sup>[15]</sup>.

## 6 Numerical simulations

A pure phase phantom was modeled and the refraction angle data were calculated directly through Snell's law. 180 views within 180 degrees with 1.0 degree interval were taken for the reconstruction. The pixel size is 20  $\mu\text{m}$ . The details of the phantom are shown in Table 1. The reconstruction results are shown in Fig. 1. As shown in Fig. 1, the DEICT-FBP and DEICT-ART reconstruction results are almost the same when the projection data are sufficient. However, at the edge of the reconstruction image, the reconstruction value of DEICT-ART is slightly lower than the result of DEICT-FBP which can be seen from Fig. 1(e).

Table 1. The phantom details.

| object | position/mm |     |     | radii/mm |     |          | $\delta$             |
|--------|-------------|-----|-----|----------|-----|----------|----------------------|
|        | $x$         | $y$ | $z$ | $x$      | $y$ | $z$      |                      |
| 1      | 0           | 0   | 0   | 5        | 5   | $\infty$ | $2.5 \times 10^{-6}$ |
| 2      | 0           | 0   | 0   | 4        | 4   | $\infty$ | $1.5 \times 10^{-6}$ |
| 3      | 0           | 1   | 0   | 3        | 2   | 2        | $2 \times 10^{-6}$   |
| 4      | -1          | 1   | 1   | 1.5      | 1.5 | 1.5      | $1.5 \times 10^{-6}$ |

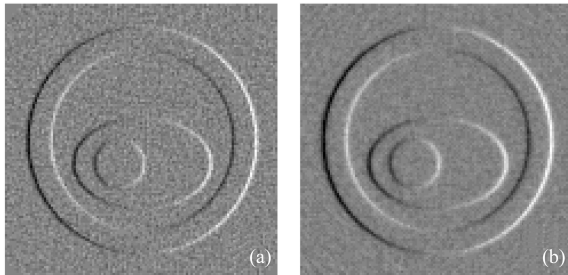


Fig. 2. Reconstruction results in a noisy circumstance, the SNR of the refraction angle data is 50 db. (a) The reconstruction result of DEICT-FBP; (b) The reconstruction result of DEICT-ART, 40 iterations.

To validate the anti-noise property of DEICT-ART algorithm, white gauss noise was added to the

refraction angle projection data of the phantom. The Signal Noise Ratio (SNR) of the generated noisy projections was 50 db. The reconstruction images are shown in Fig. 2. In a noisy circumstance, the reconstruction result of DEICT-ART is better than that of DEICT-FBP. Compared with DEICT-FBP, the result of DEICT-ART is smoother and less blurred.

As indicated in Section 1, in situations where it is not possible to measure a large number of projections or the projections are not uniformly distributed over 180° or 360°, the ART algorithm has better performances than analytical algorithm such as FBP. To simulate a few-view situation, 20 views within 180° with identical angular interval are used to do the reconstruction. Because of the simplicity of the phantom, the quality of reconstruction images is acceptable. However, strip artifacts appear due to the insufficient of the projection data. It can be seen from Fig. 3(c), in a few-view circumstance, the reconstruction result of DEICT-ART is smoother than DEICT-FBP.

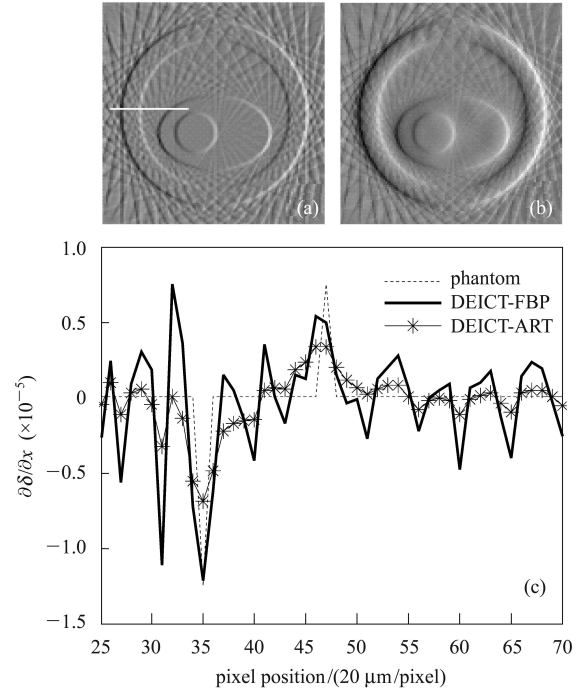


Fig. 3. Few-view reconstruction results of the phase phantom, 20 views. (a) The reconstruction result of DEICT-FBP; (b) The reconstruction result of DEICT-ART; (c) Local profile comparison of the 60th row indicated by the white line in (a).

## 7 Experiments at BSRF

The DEI-CT experiments were performed at the

4W1A Station of the BSRF. The layout of DEI-CT setup is described in Section 2. The setup was located approximately 43 m away from the source. The energy of the monochromatic X-rays was 10 keV. A plastic cylinder cut from a common ball-point pen refill was inspected in experiment, as shown in Fig. 4(a). Its outer diameter was 3 mm and its inner diameter was 1.5 mm. The pixel size was 10.9  $\mu\text{m}$ . The sample was rotated in 1.0 degree interval within 180 degrees.

For each projection direction, seven DEI images were measured at different positions of the RC. The refraction angle information was extracted by the MIS method<sup>[11]</sup>. The size of the reconstruction image is  $120 \times 120$  pixels. 20 views within 180 degrees with identical angular interval are used to simulate a few-view reconstruction. The reconstruction results are shown in Fig. 4. As shown in Fig. 4(f), in the few-view circumstance, the strip artifacts appear just as in the case of simulation. These artifacts can be eliminated or weakened by the PDE filter. In Fig. 4(g), after 2 iterations, the artifacts in the region of the rectangle are significantly weakened. It can be seen in Fig. 4(h), that the flat region of the image is smoothed while the edges are preserved.

A disadvantage of the ART iterative algorithm is that the time-consumption is far longer than analytical algorithms. To accelerate the DEICT-ART algorithm, an ordered subsets technique is adopted. 180 views from  $1^\circ$  to  $180^\circ$  are divided into 5 subsets. The residual per pixel is used as figure of merit to illuminate the convergence of the proposed DEICT-ART algorithm:

$$r^k = \frac{|x^{k+1} - x^k|}{N}, \quad (11)$$

where  $N$  is the number of pixels and  $x^k$  is the reconstruction image of the  $k$ th iteration. As shown in Fig. 5, the convergence of DEICT-OS-ART is faster than ordinary DEICT-ART especially in the incipient iterations and both of the two algorithms converge to the identical value. The time-consumption of one step iteration of DEICT-OS-ART and DEICT-ART is the same<sup>[14]</sup>, however the speed of the reconstruction can benefit from the faster convergence rate of DEICT-OS-ART. To achieve the same image quality of the reconstruction, the number of iterations needed is about 10% reduction in DEICT-OS-ART in our experiments. The time cost of one step iteration is around 0.6 second with a dual-core 1.8 G CPU and 1 G memory and the program code is implemented in Matlab currently.

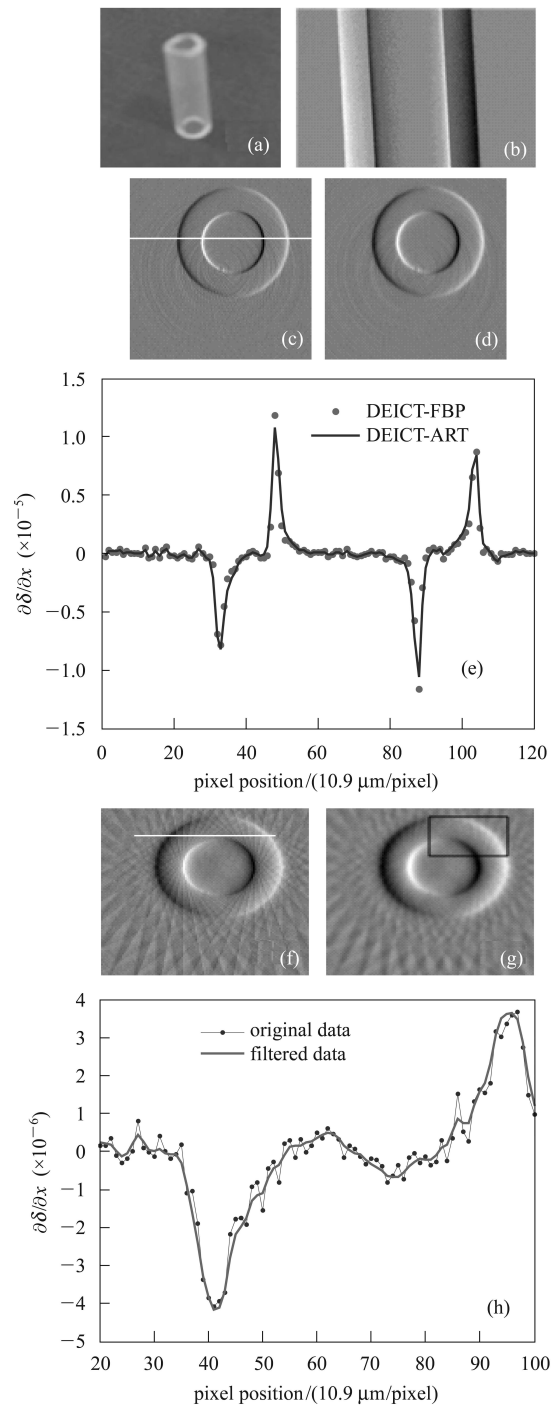


Fig. 4. Reconstruction results of the experiment data. (a) The sample, a plastic cylinder; (b) One view of the refraction-angle extracted by the MIS method; (c) The reconstruction result of DEICT-FBP; (d) The reconstruction result of DEICT-ART, 40 iterations; (e) Local profile comparison of the 60th row indicated by the white line in (c). (f) DEICT-ART reconstruction of the plastic cylinder, 20 views; (g) PDE filtering of (f), 2 iterations,  $\sigma$  of Eq. (9) is set to 0.5 and the  $\Delta t$  of Eq. (10) is set to 0.2; (h) Local profile of the 30th row indicated by the white line in (f).

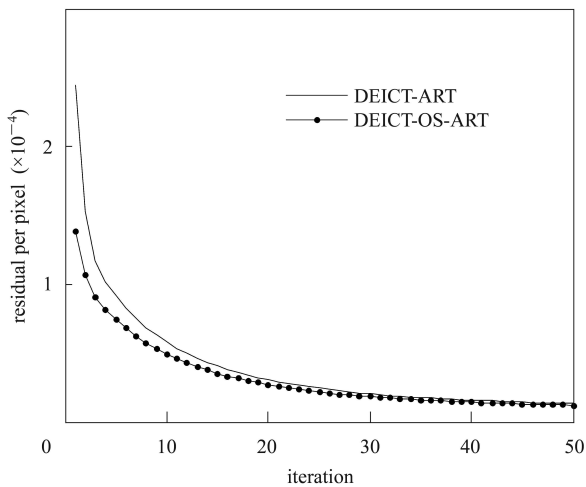


Fig. 5. The convergence curve of DEICT-ART and DEICT-OS-ART of the experiment data.

## 8 Conclusions

In this paper, an ART iterative algorithm named DEICT-ART is proposed to reconstruct the gradient of the refraction index for computer tomography of diffraction enhanced imaging. The algorithm is in the reconstruction framework of Zhu et al<sup>[6]</sup> and simply replaces the conventional FBP algorithm with an ART algorithm. In situations where the projec-

tion data are sufficient, the reconstruction results of DEICT-FBP and DEICT-ART are comparable except that at the sharp edges, the value of DEICT-ART is slightly lower than that of DEICT-FBP. In the noisy circumstance and the few-view circumstance, the DEICT-ART algorithm which inherits the advantage of ART performs better than DEICT-FBP. The reconstruction images of DEICT-ART are smoother than DEICT-FBP. In a few-view circumstance, strip artifacts seriously affect the reconstruction image quality of DEICT-ART. A new type of iterative image restoration method named PDE filter can significantly eliminate or weaken the artifacts. The PDE filter has the property of edge-preserving and denoising. Besides the proposed PDE filter method, other edge-preserving and denoising techniques can also be adapted, e.g. total variance (TV) image restoration. One disadvantage of the ART iterative algorithms is the long time-consumption. However, DEICT-ART can benefit from the ordered subsets acceleration technique. This problem can also be solved or weakened by now emerging computation technologies, such as DSP chips and GPU acceleration.

*The experiments were carried out at the BSRF, so the authors appreciate the support of the BSRF.*

## References

- 1 Chapman D, Thomlinson W, Arfelli F et al. Rev. Sci. Instrum., 1996, **67**: 3360
- 2 Dilmanian F A, ZHONG Z, REN B et al. Phys. Med. Biol., 2000, **45**: 933–46
- 3 Pavlov K M, Kewish C M, Davis J R et al. J. Phys. D: Appl. Phys., 2001, **34**: A168–72
- 4 Maksimenko A, Ando M, Hiroshi S et al. Appl. Phys. Lett., 2005, **86**: 124105
- 5 HUANG Z F, KANG K J, ZHANG Li et al. Appl. Phys. Lett., 2006, **89**: 041124
- 6 ZHU P P, WANG J Y, YUAN Q X et al. Appl. Phys. Lett., 2005, **87**: 264101
- 7 LIU Y J, ZHU P P, CHEN B et al. Phys. Med. Biol., 2007, **52**: L5-L13
- 8 ZHANG Kai, ZHU Pei-Ping, HUANG Wan-Xia et al. Acta Physica Sinica, 2008, **57**(6): 3410–3418 (in Chinese)
- 9 CHEN Z Q, DING F, HUANG Z F et al. Chin. Phys. C (HEP & NP), 2009, **33**(11): 961–966
- 10 HUANG Z F, KANG K J, ZHU P P et al. Phys. Med. Biol., 2007, **52**: 1–12
- 11 Oltulu O, ZHONG Z, Hasnah M et al. J. Phys. D: Appl. Phys., 2003, **36**: 2152–6
- 12 Gilbert P. J. Theor. Biol., 1972, **76**: 105–117
- 13 Kak A C, Slaney M. Principles of Computerized Tomographic Imaging. New York: IEEE Press, 1988
- 14 Hudson H M, Larkin R S. IEEE Trans. Med. Imaging, 1994, **13**(4): 601-9
- 15 Perona P, Malik J. IEEE Trans. Pattern Anal. Mach. Intell., 1990, **12**(7): 629-39